Chapter 2

Infrared Multiphoton Dissociation Mass Spectrometry for Structural Elucidation of Oligosaccharides

Bensheng Li, Hyun Joo An, Jerry L. Hedrick, and Carlito B. Lebrilla

Summary

The structural elucidation of oligosaccharides remains a major challenge. Mass spectrometry provides a rapid and convenient method for structural elucidation on the basis of tandem mass spectrometry. Ions are commonly selected and subjected to collision-induced dissociation (CID) to obtain structural information. However, a disadvantage of CID is the decrease in both the degree and efficiency of dissociation with increasing mass.

In this chapter, we illustrate the use of infrared multiphoton dissociation (IRMPD) to obtain structural information for *O*- and *N*-linked oligosaccharides. The IRMPD and CID behaviors of oligosaccharides are compared.

Key words: Infrared multiphoton dissociation, Oligosaccharide, Collision-induced dissociation, Cross-ring cleavage.

1. Introduction

Glycosylation is an important posttranslational modification of proteins *(1)*. Carbohydrate moieties in glycoproteins are known to mediate a number of essential functions such as protein folding *(4, 5)*, cell–cell and cell–matrix recognition, cellular adhesion, inter- and intracellular interaction, and protection *(6)*. The high complexity of glycans poses a challenge in the determination of carbohydrate structures. The conventional analysis for glycans in glycoconjugates involves a combination of techniques such as NMR, mass spectrometry (MS), chemical derivatization, and monosaccharide composition analysis *(7–10)*. Mass spectrometry

Nicolle H. Packer and Niclas G. Karlsson (eds.), *Methods in Molecular Biology, Glycomics: Methods and Protocols, vol. 534*

DOI: 10.1007/978-1-59745-022-5_2

has become a versatile analytical technique for structural characterization of small organic compounds and biomacromolecules in proteomics, glycomics, and metabolomics because of its high sensitivity, accuracy, and resolution *(11–14)*. Tandem mass spectrometry (MS^n), in which a precursor ion is mass selected, dissociated, and the product ions are analyzed, has been an essential technique for structure analysis of biomolecules. In the structure elucidation of oligosaccharides, collision-induced dissociation (CID) is the most common method to obtain sequence, connectivity, stereochemistry, and even the linkage.

Infrared multiphoton dissociation (IRMPD) is especially well suited for the dissociation of trapped ions in Fourier transform ion cyclotron resonance mass spectrometry (FTICR MS). The resonant absorption of a few IR photons with relatively low energy allows the ions of interest to be fragmented selectively along its lowest-energy dissociation pathways. In an IRMPD event, a precursor ion of interest is mass-selected and trapped in the analyzer cell, dissociated by absorption of IR photons, and the product ions are analyzed for structural information. There are some advantages of IRMPD over other MS^n techniques, such as CID. Most organic molecules are IR active and readily absorb IR photons. In contrast to CID, no collision gas is needed for the dissociation of precursor ions, thus shortening the analysis time. IR photon absorption does not cause translational excitation of ions as CID does, therefore minimizing ion losses due to ejection or ion scattering. Moreover, since both the precursor and product ions absorb IR photons, more extensive fragmentation occurs to yield richer structural information. With IRMPD, ions are fragmented on-axis, yielding more efficient observation of product ions. IRMPD also provides better control of excitation energy with minimal mass discrimination. IRMPD has been extensively applied with FTICR-MS for the structural characterization of intact proteins *(15–18)*, peptides *(19–23)*, oligonucleotides *(24–26)*, and oligosaccharides *(27–29)*.

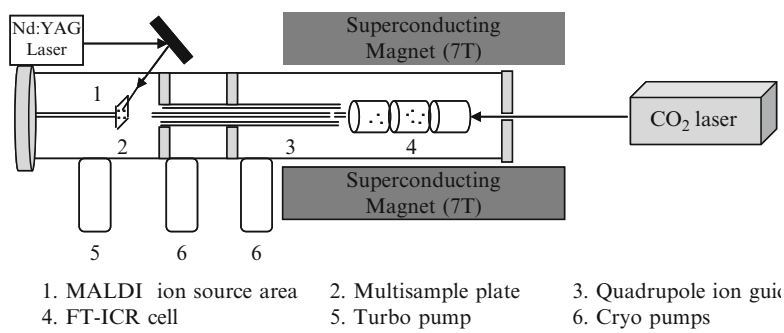

Fig. 1. A schematic assembly of MALDI-FTICR mass spectrometer coupled with a CO_2 infrared laser for IRMPD.

2. Materials

2.1. Release and Purification of Oligosaccharides

1. Materials for release of *O*-linked oligosaccharides, *see* the Chapter 10 "Collision-Induced Dissociation Tandem Mass Spectrometry for Structural Elucidation of Glycans.
2. PNGase F (NEW ENGLAND BioLabs).
3. *N*-linked release solution: 100 mM NH_4HCO_3, pH 7.5.
4. Heating block 37°C.
5. Ethanol.
6. Nonporous graphitized carbon and solutions to clean up oligosaccharides as described in the Chapter 10 "Collision-Induced Dissociation Tandem Mass Spectrometry for Structural Elucidation of Glycans.

2.2. HPLC Separation of Oligosaccharide Components

1. Hypercarb porous graphitized carbon (PGC) column (2.1 × 100 mm, 5 μm, ThermoQ Hypersil Division, Bellfonte, PA).
2. Solvent A (neutral oligosaccharides): H_2O.
3. Solvent B (neutral oligosaccharides): acetonitrile (AcN) containing 0.05% (v/v) trifluoroacetic acid (TFA).
4. Gradient HPLC pump (up to 250 μL/min) with photo diode-array (PDA) detector (206 nm).
5. Fraction collector with 1.5-mL microcentrifuge tubes.

2.3. MALDI-FTICR MS Analyses of Oligosaccharides

1. A commercial MALDI-FT mass spectrometer (IonSpec, Irvine, CA) with an external ion source was used to perform the analysis. The instrument is equipped with a 7.0-T shielded, superconducting magnet and a Nd:YAG laser at 355 nm.
2. MALDI matrix solution: 0.4 M 2,5-dihydroxybenzoic acid (DHB), in 50:50 H_2O/AcN.
3. Positive ion dopant: 0.1 M NaCl in 50:50 H_2O/AcN
4. MALDI stainless steel target plate.

2.4. Infrared Multiphoton Dissociation

1. A continuous-wave, turn-key 25 Watt CO_2 laser; PLX25-s, Parallax Technology, Inc. (Waltham, MA, USA).
2. 2× beam expander from Synrad, Inc. (Mukilteo, WA, USA).

3. Methods

3.1. Release and Purification of Oligosaccharides

1. The release and purification of *O*-linked oligosaccharides from glycoproteins were performed by using a method developed in the laboratory. Briefly, a certain amount of glycoprotein was treated with 1.0 M $NaBH_4$ and 0.1 M NaOH at 42 °C for 24 h,

followed by neutralization with precooled 1.0 M hydrochloric acid to a pH of 2 to get rid of the excess $NaBH_4$ in an ice bath *(30, 31)*.

2. All *N*-linked oligosaccharides were released by incubating the glycoproteins with PNGase F (1 U) in 100 mM NH_4HCO_3 (pH 7.5) for 12 h at 37 °C. The reaction mixture was boiled in water bath for 5 min to stop the reaction, followed by ethanol addition to get a 90% aqueous ethanol solution. Then, reaction mixture was chilled at –20 °C for 30 min and centrifuged. The supernatant was recovered and dried. The residue from the dried supernatant was redissolved in nanopure water for purification.
3. The resulting *O*- or *N*-linked oligosaccharide mixtures were desalted and purified by the solid-phase extraction (SPE) using nonporous graphitized carbon cartridge. The purified oligosaccharides were subjected to HPLC or MALDI-FTICR mass spectrometry.

3.2. HPLC Separation of Oligosaccharide Components

1. Oligosaccharide mixtures purified from SPE were further purified by the separation with HPLC on a Hypercarb porous graphitized carbon (PGC) column.
2. For neutral oligosaccharide separation, the solvent A was H_2O and solvent B was acetonitrile (AcN) containing 0.05% (v/v) trifluoroacetic acid (TFA). The gradient elution system was 5% to 16% of B during the first 44 min, 16–28% of B during the following 12 min (44–56 min), 28–32% of B during the next 13 min (56–69 min), 32% of B during 69–80 min, and finally followed by 5-min of elution with the solvent B down to 5%. The flow rate was set to 250 μL/min for the HPLC separation. The effluents were monitored at 206 nm by a photo diode-array (PDA) detector and collected into 1.5 mL microcentrifuge tubes at 1-min intervals.
3. Each fraction was analyzed with MALDI-FTICR for oligosaccharides after solvent evaporation.

3.3. MALDI-FTICR MS Analyses of Oligosaccharides

1. MALDI sample was prepared by loading 1–6 μL of analyte and 1 μL of matrix solution on a stainless steel target plate. For the positive mode analyses, 1 μL of 0.1 M NaCl in 50:50 H_2O/AcN was applied to the spot to enrich the Na^+ concentration and thus produce the primarily sodiated signals.
2. The plate was placed in ambient air to dry the sample spots before insertion into the ion source.

3.4. Infrared Multiphoton Dissociation

1. The CO_2 laser was installed at the rear of the superconducting magnet to provide infrared photons for IRMPD. The schematic instrument assembly is shown in **Figure 1**.
2. The laser has a working wavelength of 10.6 μm (0.1 eV per photon) and a beam diameter of 6 mm as specified by the

manufacturer. A beam expander was used to expand the laser beam to 12 mm.

3. To perform IRMPD experiments, some modifications were made on the ICR cell and the vacuum chamber. The original trapping plate with the electron filament was removed and replaced with a copper plate with a 13-mm hole in the center. Four copper wires (0.24 gauge) were fixed by screws onto the plate, two horizontally and two vertically, over the hole and set 3.6 mm apart. The existing aluminum vacuum chamber was replaced with a smaller-diameter (101.6 mm OD) tube containing a 70-mm BaF_2 window (Bicron Corp., Newbury, OH, USA).
4. The infrared laser was aimed directly toward the center of the analyzer cell. Ions were subsequently irradiated with an IR laser pulse lasting between 200 and 3,000 ms.

3.5. Interpretation of IRMPD Spectra for O-Linked Glycans

It is not often possible to collect a single oligosaccharide from complex mixtures even with HPLC separation. A fraction from a mixture of glycans obtained from the egg jelly glycoproteins of *X. borealis* may contain a number of oligosaccharides. **Figure 2** shows a typical MALDI-FT mass spectrum of a single HPLC fraction. Four major components were obtained with *m/z* 878.311,

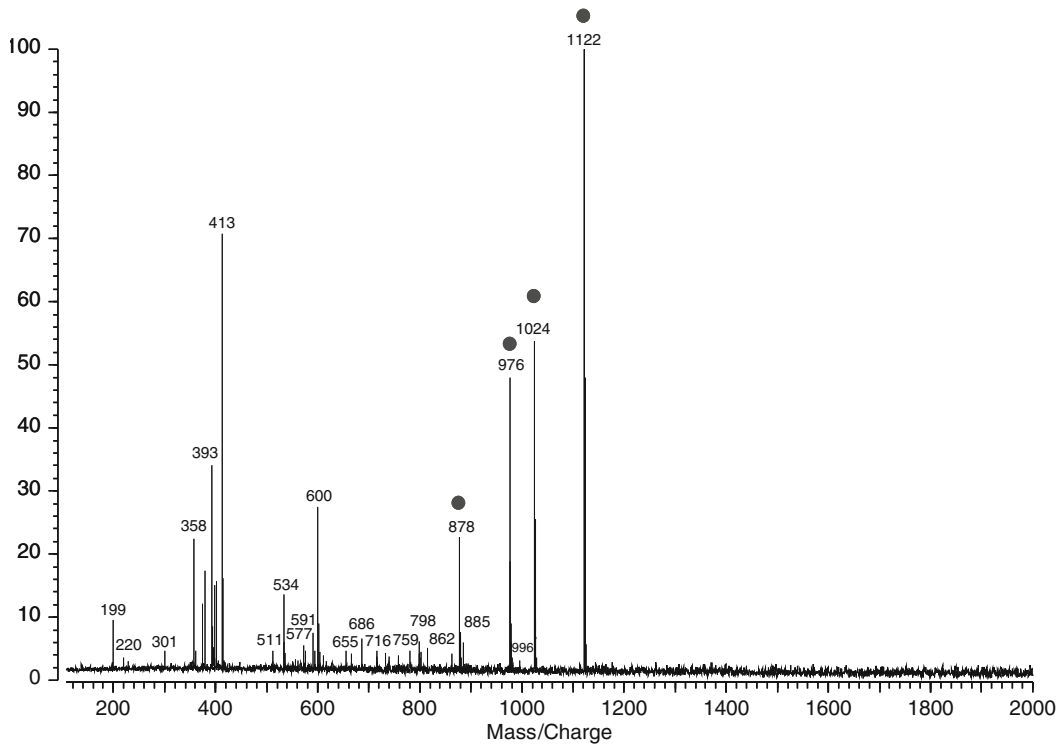

Fig. 2. MALDI mass spectrum (signals are due to sodium-coordinated species) of one HPLC fraction containing several *O*-linked oligosaccharides released from the egg jelly coat of *X. borealis*. *O*-glycans are marked by *filled circles*.

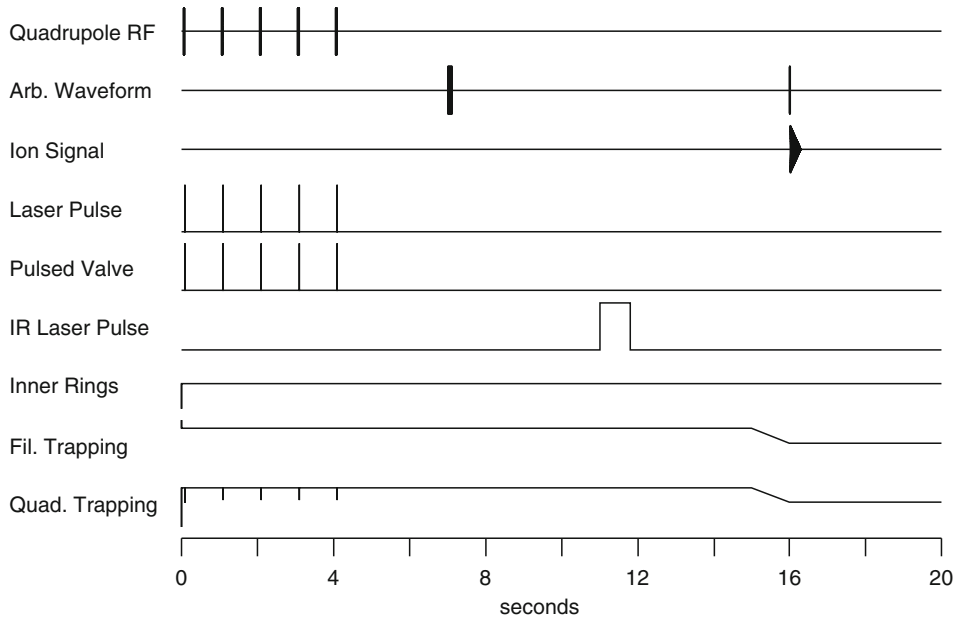

Fig. 3. A typical pulse sequence employed for IRMPD in an FTICR mass spectrometer.

976.360, 1,024.375, and 1,122.421. On the basis of the exact mass, monosaccharide compositions for each component were obtained. The sequence of each component was determined by IRMPD as shown below.

Figure 3 shows a typical pulse sequence for MALDI-IRMPD analysis. The Nd:YAG laser was fired five times at 1,000-ms intervals to get enough ions in the ICR cell. A desired ion is readily selected in the analyzer with the use of an arbitrary waveform generator and a frequency synthesizer. The CO_2 infrared laser was typically fired at 11,000 ms with a duration of 200–3,000 ms depending on the molecular size and structure of the target ion while the trapping plates were elevated to +4 V. The voltages on the trapping plates were then ramped down to + 1.2 V from 15,000 to 16,000 ms for detection.

The resulting spectra are shown in **Fig. 4**. A single component (*m/z* 1,024.375) was isolated from the *O*-glycan mixture of an HPLC fraction (**Fig. 2**) by ejecting all other ions from the ICR cell (**Fig. 4A**). After absorption of IR photons, the selected ions were fragmented into product ions as shown in **Fig. 4B**. The composition was determined based on the exact mass to correspond to three hexoses (Hex), two deoxyhexoses (dHex), and one *N*-acetylhexosamine (HexNAc) (theoretical mass 1,024.369 Da, experimental mass 1,024.375 Da, Δm = 0.006 or 6 ppm).

The primary monosaccharide sequence was elucidated from the IRMPD spectrum. The loss of a dHex (*m/z* 878), a Hex (*m/z* 862) or HexNAc-ol (the reduced HexNAc, *m/z* 801)

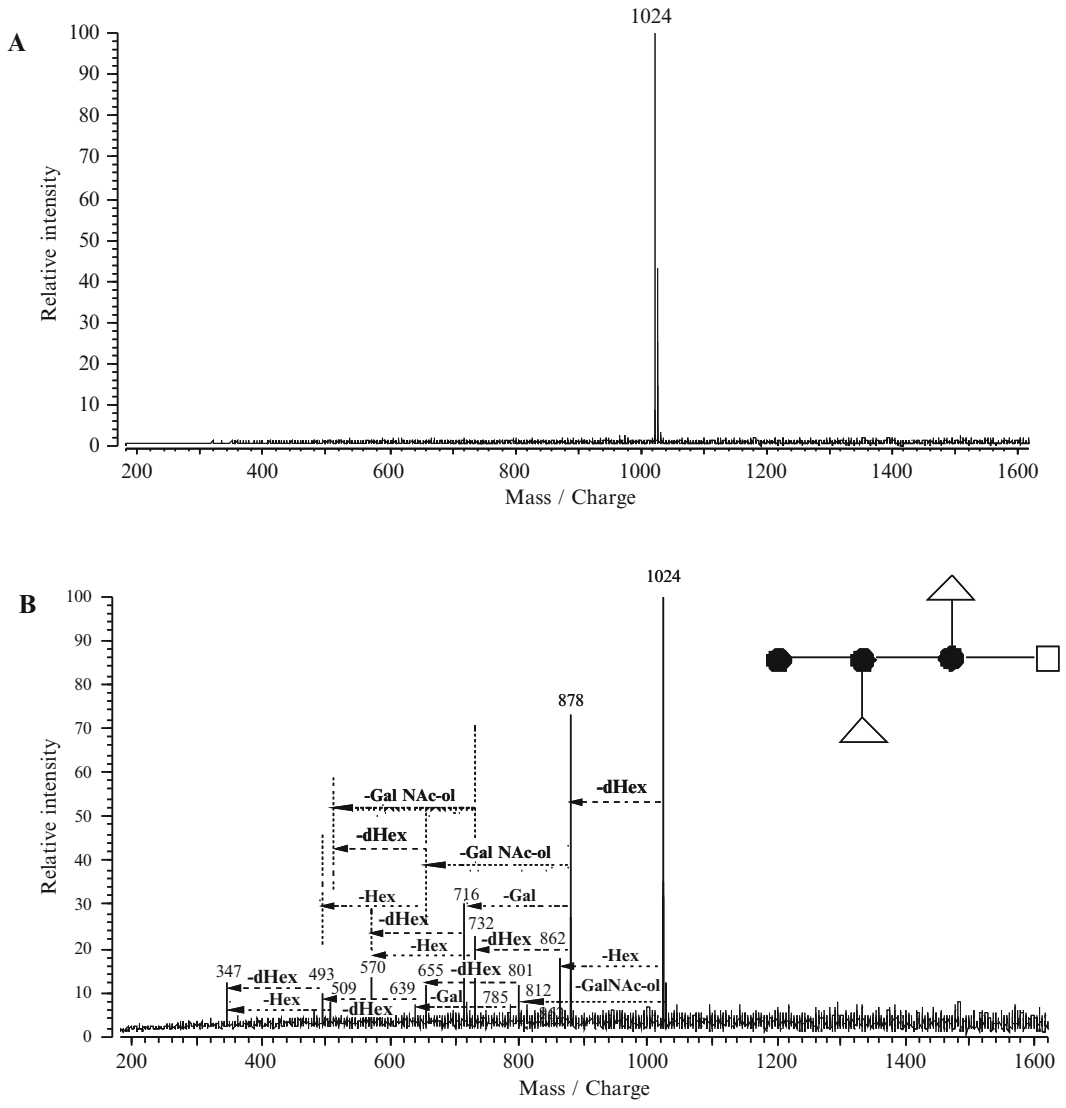

Fig. 4. The sequence of an *O*-linked glycan (*m/z* 1,024, $[M + Na]^+$) released from glycoprotein of *X. borealis* egg jelly was determined primarily by IRMPD. (**A**) The precursor ion (*m/z* 1,024) was selected and isolated from all other ions. (**B**) The ion was fragmented by absorption of IR photons over 1 s with laser power of 12.7 W. *Filled circle* Hex; *open square* GalNAc-ol; *open triangle* dHex.

indicates that the three residues are in terminal positions. The HexNAc-ol is the reducing end and is putatively a GalNAc-ol. The other two residues are in the nonreducing ends indicating at least one branched point. The ion with *m/z* 862 can lose one dHex (*m/z* 716) or one GalNAc-ol (*m/z* 639), but no further loss of one Hex was observed (*m/z* 700 not present) suggesting that at least one dHex is attached to a second Hex that is internal. The ion with *m/z* 639 loses only one dHex (*m/z* 493) with no further loss of the second Hex indicating that the other

dHex must be connected to a third internal Hex. The primary sequence of the precursor ion (*m/z* 1,024) can be deduced as being Hex–Hex(dHex)–Hex(dHex)–GalNAc-ol. The remainder of the fragment ions are internal fragments that are consistent with the proposed structure (inset of **Fig. 4B**).

Another oligosaccharide component in the HPLC fraction with a mass of *m/z* 1,122.421 (*see* **Fig. 2**) was also subjected to IRMPD. On the basis of the exact mass, the ion consists of two hexoses (Hex), one deoxyhexose (dHex), and three *N*-acetyl hexosamines (HexNAc) (theoretical mass 1,122.417 Da, experimental mass 1,122.421 Da, m = 0.004 or 4 ppm). The IRMPD spectrum of isolated *m/z* 1,122 is shown in **Fig. 5**. The quasimolecular ion $[M + Na]^+$ loses a single dHex (*m/z* 976) followed by the loss of one Hex (*m/z* 814) indicating that the previously lost dHex is attached to a Hex residue at the nonreducing end. There is no Hex loss (*m/z* 960) from the quasimolecular ion suggesting that there is no Hex at the nonreducing end. The ion *m/z* 814 loses either one Hex (*m/z* 652), one GalNAc-ol (*m/z* 591), or one HexNAc (*m/z* 611). It is noted that the loss of GalNAc-ol or the loss of HexNAc from the same precursor ion *m/z* 814 occurs by two separate pathways, namely, the former follows the loss of the Hex connecting to reducing end and the latter is preceded

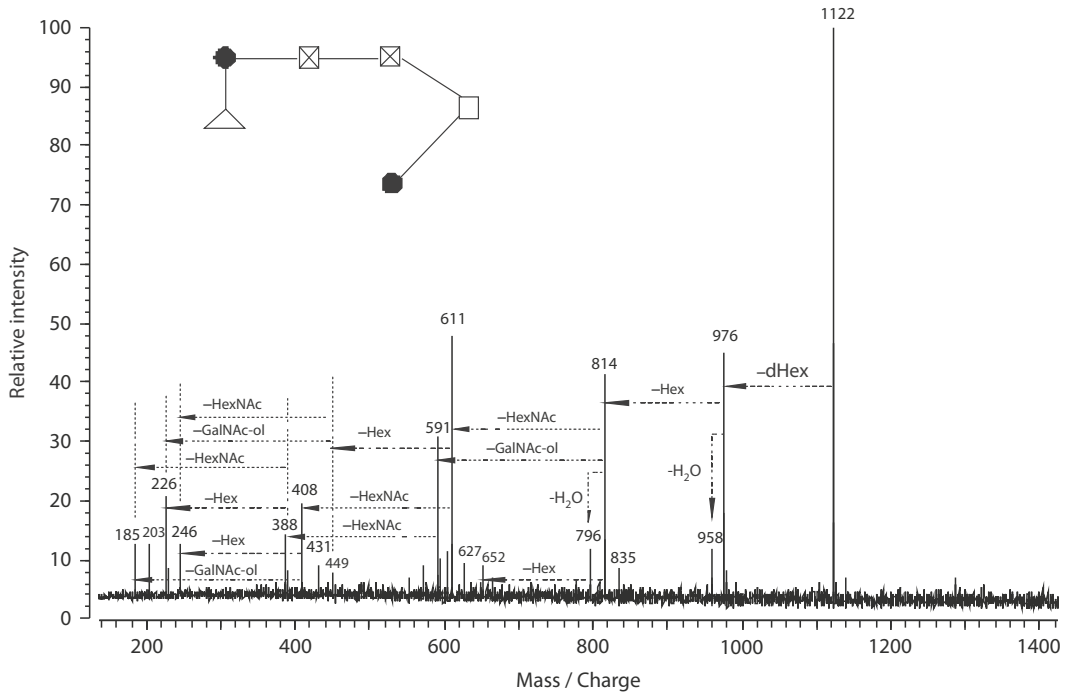

Fig. 5. IRMPD spectrum of an *O*-linked oligosaccharide with *m/z* 1,122 ($[M + Na]^+$, see Fig. 2). The IR laser was fired for 1 s with laser power setting at 12.7 W. The primary component sequence of the *O*-linked glycan was determined based on the spectrum and shown in the *inset*. *Filled circle* Hex; *open square* GalNAc-ol; *open triangle* dHex; *crossed square* HexNAc.

by the loss of the other internal Hex. There is another HexNAc loss (*m/z* 408) from the ion *m/z* 611, which comes directly from *m/z* 814 through the loss of one HexNAc, thus indicating that the two HexNAc are connected to each other. On the basis of the above information, the primary sequence of the ion *m/z* 1,122 is determined as shown in the inset of **Fig. 5**.

The sequence is further confirmed by the additional fragments. The ion *m/z* 611 loses one Hex (*m/z* 449) corresponding to HexNAc-GalNAc-ol, or one HexNAc to yield Hex-GalNAc-ol (*m/z* 408). The ion *m/z* 449 loses either one HexNAc to yield a GalNAc-ol (*m/z* 246) or one GalNAc-ol to produce a HexNAc (*m/z* 226). The *m/z* 408 ion is fragmented into two ions to yield either a Hex (*m/z* 185) or a GalNAc-ol (*m/z* 246). In addition, the ion *m/z* 591, Hex–HexNAc–HexNAc, loses one HexNAc to yield Hex–HexNAc (*m/z* 388), which then loses one Hex to yield a HexNAc (*m/z* 226) (*see* **Note 1**).

3.6. Interpretation of IRMPD Spectra for N-Linked Glycans

A common problem with CID for large molecules is the lack of fragments so that MS^n ($n > 2$) is required to obtain the complete sequence. IRMPD requires only a single MS/MS event to obtain the complete sequence resulting in greater sensitivity (better signal-to-noise).

As an example, a high-mannose type *N*-linked glycan consisting of two GlcNAc and nine mannoses (Man9) was examined *(32)*. The IRMPD spectrum of the quasimolecular ion (*m/z* 1,905.634, $[M + Na]^+$) is shown in **Fig. 6B**. The extensive fragmentation was observed in a single MS/MS event. In the contrast, the CID of this compound (**Fig. 6A**) did not produce the complete sequence even after MS^3 at which point the signal was lost. For *N*-linked glycans, the putative structure can be deduced based on the composition.

Often the goal of tandem MS is to confirm the putative structure and obtain linkage information. The CID and IRMPD of Man9 are compared in **Fig. 6**. Large fragment ions were obtained corresponding to the B_5 and B_4 fragments (*m/z* 1,685 and 1,481, respectively) in the CID. Subsequent mannose losses from B_4 ion were clearly discernable (*m/z* 1,319, 1,157, 995, 833, 671, and 509), but no series of mannose losses from B_5 were observed. In addition, a number of cross-ring cleavages were observed. These ions originated from the internal cleavage of the major branching mannose ($^{0,3}A_4$, *m/z* 923) and the subsequent mannose losses from the $^{0,3}A_4$ fragment ($^{0,3}A_4/Y_{5\alpha}$, *m/z* 761; $^{0,3}A_4/Y_{5\alpha}$, *m/z* 599; $^{0,3}A_4/Y_{4\alpha',5\alpha}$, *m/z* 437, respectively). A minor fragment corresponding to $^{0,4}A_4/Y_{5\alpha'}$ was also observed (*m/z* 731) with an accompanying mannose loss ($^{0,4}A_4/Y_{5\alpha}$, *m/z* 569). The cross-ring cleavages were limited, but provided information regarding the first branched residue and the linkages of the antennae.

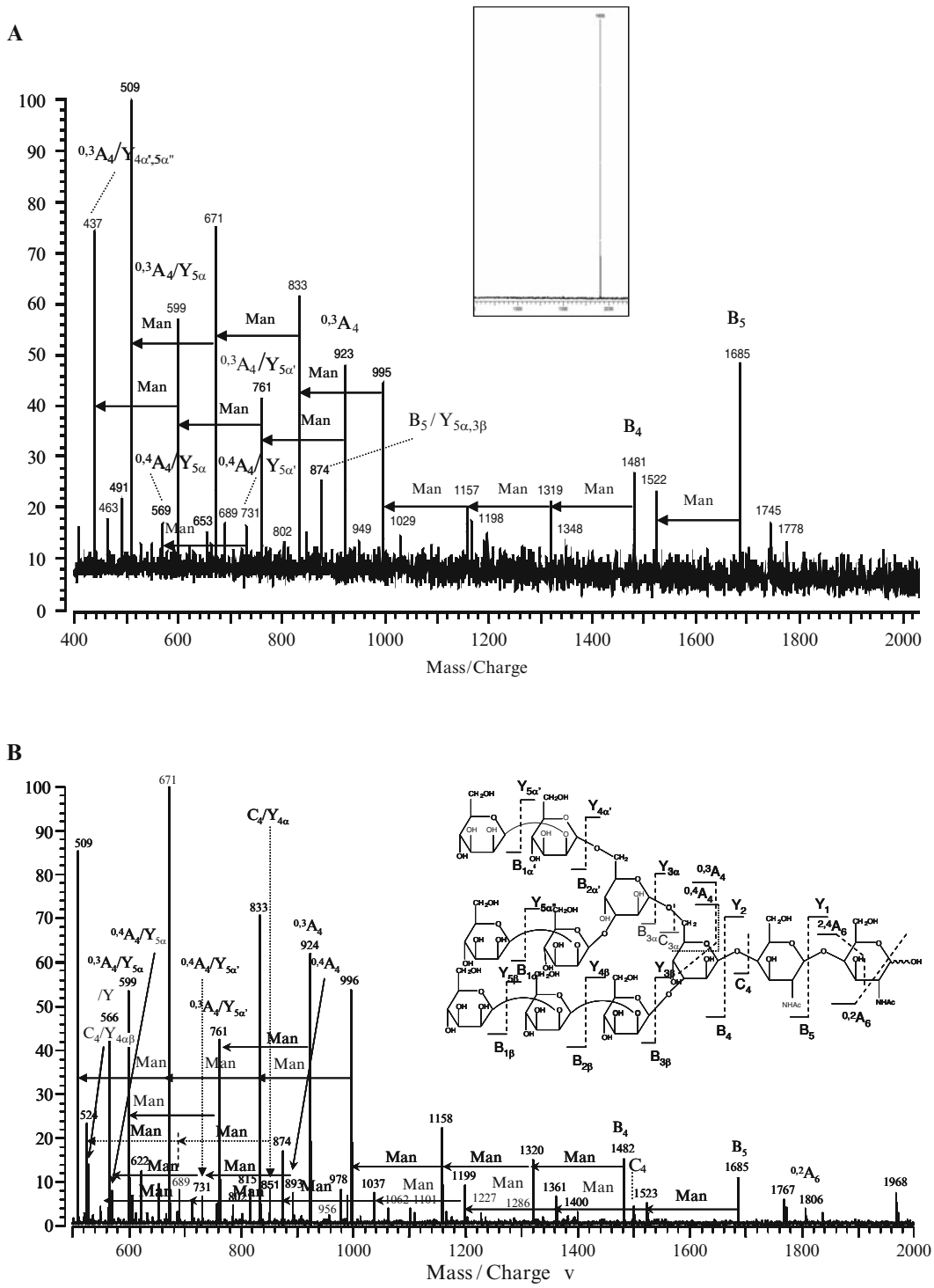

Fig. 6. (**A**) CID and (**B**) IRMPD spectra of *N*-linked oligosaccharide Man9. The spectra show cross-ring cleavages with some branching information as well as B and Y fragments. The inset of (**B**) shows the structure of Man9 with labeled fragmentations.

The IRMPD spectrum of Man9 (**Fig. 6B**) showed significantly more structural information and better signal-to-noise ratio. A fragment ion, $^{0,2}A_6$, corresponding to the cross-ring cleavage of the reducing end, was the largest fragment ion detected (*m/z* 1,806). The B_5 and B_4 ions (*m/z* 1,685 and 1,482, respectively) were readily observed along with fragments corresponding to subsequent mannose losses, respectively. The extensive fragmentation represents a major difference between the CID and IRMPD spectra. The mannose losses from the B_5 ion were incomplete in the CID spectrum (**Fig. 6A**), while both B_4 and B_5 showed the subsequent mannose losses in the IRMPD spectrum. The results demonstrate that with IRMPD essentially every glycosidic bond cleavage is represented while ion loss is minimized.

Another ion that was not observed in the CID spectrum is the C_4 fragment (*m/z* 1,499) and subsequent losses of mannose (C_4/Y_n). These ions were present in IRMPD spectrum at *m/z* 1,337, 1,175, 1,013, 851, 689, and 527. Some internal fragments were also present in the IRMPD spectrum, but not in the CID spectrum. These fragments corresponded to products of cross-ring cleavages occurring at the core branching mannose. These ions were present at *m/z* 893, 731, and 569 and corresponded to the $^{0,4}A_4$ ion and those with subsequent mannose losses, respectively. Another series of cross-ring cleavages representing the $^{0,3}A_4$ fragment from the same mannose core with subsequent mannose losses (*m/z* 923, 761, and 599) were observed and were more intense than the $^{0,4}A_4$ series. The fragmentation patterns observed in the IRMPD spectrum provided substantial information for the structural elucidation of $GlcNAc_2Man_9$ compared to the CID (*see* **Note 2**).

4. Notes

1. The primary sequence of *O*-linked glycans could be determined based solely on IRMPD analysis. However, their linkages and anomeric characters could not be determined. A method for obtaining this information as well as the identity of the residue involving the use of exoglycosidases with IRMPD or CID has been published previously *(30)*.
2. Owing to the symmetric nature of the antennae for Man9, there are several peaks in the CID (**Fig. 6A**) and IRMPD (**Fig. 6B**) that could be attributed to several cleavages. For simplicity, only a single assignment is provided for each cleavage.

Acknowledgements

The authors gratefully acknowledge the financial support from the National Institutes of Health (R01 GM049077).

References

1. Apweiler, R., Hermjakob, H. and Sharon, N. (1999) On the frequency of protein glycosylation, as deduced from analysis of the SWISS-PROT database. *Biochim. Biophys. Acta* 1473, 4–8.
3. Moens, S. and Vanderleyden J. (1997) Glycoproteins in prokaryotes. *Arch. Microbiol.* 168, 169–175.
4. Cyster, J. G., Shotton, D. M. and Williams, A. F. (1991) The dimensions of the T lymphocyte glycoprotein leukosialin and identification of linear protein epitopes that can be modified by glycosylation. *EMBO J.* 10, 893–902.
5. Helenius, A. and Aebi, M. (2001) Intracellular Functions of N-Linked Glycans. *Science* 291, 2364–2369.
6. Varki, A. (1993) Biological roles of oligosaccharides: all of the theories are correct. *Glycobiology* 3, 97–130.
7. Carpita, N.C., Shea, E.M., Niermann, C.J. and McGinnis, G.D., Eds. (1989) *Analysis of Carbohydrates by GLC and MS;* CRC: Boca Raton, FL, pp 151–216.
8. Hellerqvist, C. G. (1990) Linkage analysis using lindberg method. *Methods Enzymol.* 193, 554–573.
9. Mukerjea, R., Kim, D. and Robyt, J. F. (1996) Simplified and improved methylation analysis of saccharides, using a modified procedure and thin-layer chromatography. *Carbohydr. Res.* 292, 11–20.
10. Solouki, T., Reinhold, B. B., Costello, C. E., O'Malley, M., Guan, S. and Marshall, A. G. (1998) Electrospray ionization and matrix-assisted laser desorption/ionization Fourier transform ion cyclotron resonance mass spectrometry of permethylated oligosaccharides. *Anal. Chem.* 70, 857–864.
11. Song, A., Zhang, J., Lebrilla, C. B. and Lam, K. S. (2004) Solid-phase synthesis and spectral properties of 2-Alkylthio-6H-pyrano[2,3-f]benzimidazole-6-ones: A Combinatorial approach for 2-Alkylthioimidazocoumarins. *J. Comb. Chem.* 6(4), 604–610.
12. Skop, A. R., Liu, H., Yates, J. R., Meyer, B. J. and Heald, R. (2004) Functional proteomic analysis of the mammalian midbody reveals conserved cell division components, *Science* 305, 61–66.
13. An, H. J., Miyamoto, S., Lancaster, K. S., Kirmiz, C., Li, B., Lam, K. S., Leiserowitz, G. S. and Lebrilla, C. B. (2006) Global profiling of glycans in serum for the diagnosis of potential biomarkers for ovarian cancer. *J. Proteome Res.* 5, 1626–1635 (Web release at 05–27–2006).
14. Des Rosiers, C., Lloyd, S., Comte, B. and Chatham, J. C. (2004) A critical perspective of the use of 13C-isotopomer analysis by GCMS and NMR as applied to cardiac metabolism. *Metab. Eng.* 6, 44–58.
15. Little, D. P., Speir, J. P., Senko, M. W., O'Connor, P. B. and McLafferty, F. W. (1994) Infrared multiphoton dissociation of large multiply charged ions for biomolecule sequencing. *Anal. Chem.* 66, 2809–2815.
16. Mortz, E., O'Connor, P. B., Roepstorff, P., Kelleher, N. L., Wood, T. D., McLafferty, F. W. and Mann, M. (1996) Sequence tag identification of intact proteins by matching tandem mass spectral data against sequence data bases. *Proc. Natl. Acad. Sci. U.S.A.* 93, 8264–8267.
17. Li, W., Hendrickson, C. L., Emmett, M. R. and Marshall, A. G. (1999) Identification of intact proteins in mixtures by alternated capillary liquid chromatography electrospray ionization and LC ESI infrared multiphoton dissociation fourier transform ion cyclotron resonance mass spectrometry. *Anal. Chem.* 71, 4397–4402.
18. Meng, F., Cargile, B. J., Patrie, S. M., Johnson, J. R., McLoughlin, S. M. and Kelleher, N. L. (2002) Processing complex mixtures of intact proteins for direct analysis by mass spectrometry. *Anal. Chem.* 74, 2923–2929.
19. Jockusch, R. A., Paech, K. and Williams, E. R. (2000) Energetics from slow infrared multiphoton dissociation of biomolecules. *J. Phys. Chem. A* 104, 3188–3196.
20. Masselon, C., Anderson, G. A., Harkewicz, R., Bruce, J. E., Pasa-Tolic, L. and Smith, R. D. (2000) Accurate mass multiplexed tandem mass spectrometry for high-throughput polypeptide identification from mixtures. *Anal. Chem.* 72, 1918–1924.

21. Flora, J. W. and Muddiman, D. C. (2001) Selective, sensitive, and rapid phosphopeptide identification in enzymatic digests using ESI-FTICR-MS with infrared multiphoton dissociation. *Anal. Chem.* 73, 3305–3311.
22. Hakansson, K., Cooper, H. J., Emmett, M. R., Costello, C. E., Marshall, A. G. and Nilsson, C. L. (2001) Electron capture dissociation and infrared multiphoton dissociation MS/MS of an N-glycosylated tryptic peptide to yield complementary sequence information. *Anal. Chem.* 73, 4530–4536.
23. Li, L., Masselon, C. D., Anderson, G. A., Pasa-Tolic, L., Lee, S. W., Shen, Y., Zhao, R., Lipton, M. S., Conrads, T. P., Tolic, N. and Smith, R. D. (2001) High-throughput peptide identification from protein digests using data-dependent multiplexed tandem FTICR mass spectrometry coupled with capillary liquid chromatography. *Anal. Chem.* 73, 3312–3322.
24. Little, D. P. and McLafferty, F. W. (1995) Sequencing 50-mer DNAs using electrospray tandem mass spectrometry and complementary fragmentation methods. *J. Am. Chem. Soc.* 117, 6783–6784.
25. Little, D. P., Aaserud, D. J., Valaskovic, G. A. and McLafferty, F. W. (1996) Sequence information from 42–108-mer DNAs (complete for a 50-mer) by tandem mass spectrometry *J. Am. Chem. Soc.* 118, 9352–9359.
26. Little, D. P. and McLafferty, F. W. (1996) Infrared photodissociation of non-covalent adducts of electrosprayed nucleotide ions. *J. Am. Soc. Mass Spectrom.* 7, 209–210.
27. Xie, Y. and Lebrilla, C. B. (2003) Infrared multiphoton dissociation of alkali metal-coordinated oligosaccharides. *Anal. Chem.* 75, 1590–1598.
28. Zhang, J., Schubothe, K., Li, B., Russell, S. and Lebrilla, C. B. (2005) Infrared multiphoton dissociation of *O*-linked mucin-type oligosaccharides. *Anal. Chem.* 77, 208–214.
29. Goldberg, D., Bern, M., Li, B. and Lebrilla, C. B. (2006) Automatic determination of *O*-glycan structure from fragmentation spectra. *J. Proteome Research* 5, 1429–1434.
30. Zhang, J., Lindsay, L. L., Hedrick, J. L. and Lebrilla, C. B. (2004) Strategy for profiling and structure elucidation of mucin-type oligosaccharides by mass spectrometry. *Anal. Chem.* 76, 5990–6001.
31. Tseng, K., Hedrick, J. L. and Lebrilla, C. B. (1999) Catalog-library approach for the rapid and sensitive structural elucidation of oligosaccharides. *Anal. Chem.* 71, 3747–3754.
32. Lancaster, K. S., An, H. J., Li, B. and Lebrilla, B. C. (2006) Interrogation of *N*-linked oligosaccharides using infrared multi-photon dissociation in FT-ICR mass spectrometry. *Anal. Chem.* 78 (14), 4990–4997.